Journal of Cosmetic Dermatology

WILEY

JCD Journal of Cosmetic Dermatology

ORIGINAL ARTICLE OPEN ACCESS

Inhibitory Effects of Litchi Extract on Sebum Secretion and Its Mechanism: Evidence From a Mouse Model and Sebaceous Gland Cell Transcriptomics

Qinqian Tao[1] | Xingmei Chen[1] | Xian Chen[2] | Xiang Yang[2] | Erping Yan[1]

[1]Guangdong Kangaroo Mommy Group Co., Ltd., Guangzhou, China | [2]Eneplus Biotech Co., Ltd., Guangzhou, China

Correspondence: Erping Yan (jsyan6944@icloud.com)

Received: 16 December 2025 | **Revised:** 14 May 2026 | **Accepted:** 26 May 2026

Keywords: *Litchi chinensis* | mouse experiment | RNA sequencing | skin oil control | total flavonoids

ABSTRACT

Objective: Acne vulgaris is one of the most common chronic inflammatory dermatological disorders, affecting 85%–100% of adolescents and persisting into adulthood for a significant portion of the population. *Litchi chinensis*, a subtropical fruit originating from Southern China and famously associated with the Guangzhou region, is commercially significant worldwide. Recent studies have highlighted the diverse bioactivities of it and its potential for skin health. However, its oil-control properties remain unexplored.

Methods: Herein, total polyphenols, flavonoids, and polysaccharides were extracted and enriched from *L. chinensis* using various extraction processes. Their effect on skin inflammation and water–oil imbalance was subsequently evaluated in a mouse model of seborrheic dermatitis.

Results: *Litchi chinensis* flavonoids (LCFs) markedly mitigated inflammatory symptoms and restored water–oil homeostasis in mice with mixed contact dermatitis. Then we detected LCFs by high performance liquid chromatography (HPLC) and found that it mainly contains rutin, quercitrin, luteoloside, naringin, isoquercitrin, and phroridzin. Sebaceous gland cell transcriptomics revealed that LCFs modulated key genes involved in fatty acid metabolism and degradation, insulin resistance, PI3K-Akt and AMPK signaling, and triglyceride metabolism in linoleic acid-stimulated sebaceous gland cells. Based on the results of transcription group, we tested the function and found that the inhibition rate of LCFs group on oil secretion was 32.162%, which had an obvious oil control effect.

Conclusion: These findings indicate that *L. chinensis* flavonoids suppress excessive sebum secretion through multiple molecular pathways, offering novel mechanistic insights and a promising basis for developing oil-control skincare products.

1 | Introduction

The skin, as the largest organ of the human body, is coated by a physiological lipid film primarily composed of sebum secreted by sebaceous glands, epidermal lipids, and sweat [1]. This lipid layer plays a pivotal role in preserving the integrity of the skin barrier, maintaining epidermal hydration, and providing protection against microbial colonization, thereby serving as the first

Abbreviations: ACC, Akt kinase (protein kinase B); ACLY, ATP-citrate lyase; AGPAT, Acyl-glycerol-3-phosphate acyltransferase; AKT1, Akt kinase (protein kinase B) 1; AKT2, Akt kinase (protein kinase B) 2; AMPK, Adenosine 5′-monophosphate (AMP)-activated protein kinase; CPT1, Carnitine acyl-transferase 1; DHT, Dihydrotestosterone; FASN, Fatty acid synthase; FGFR1, Fibroblast growth factor receptor 1; FGFR3, Fibroblast growth factor receptor 3; FoxO1, Forkhead box O1; IL-1β, Interleukin-1β; INSR, Insulin receptor; JNK, c-Jun N-terminal kinase; MAPK, Mitogen-activated protein kinase; MMP-2, Matrix metallopeptidase 2; mTORC1, Mechanistic target of rapamycin complex 1; mTORC2, Mechanistic target of rapamycin complex 2; PI3K, Phosphoinositide 3-kinase; SCD1, Stearoyl-CoA desaturase-1; SESN2, Sestrin 1; SLC27A1, Solute carrier family 27 member 1; SRD5A1, Steroid 5 alpha-reductase 1; SRD5A2, Steroid 5 alpha-reductase 2; SREBF1, Sterol regulatory element-binding transcription factor 1; SREBP1, Sterol regulatory element-binding protein 1; TRP-2, Tyrosinase-related protein 2; TSLP, Thymic stromal lymphopoietin.

This is an open access article under the terms of the Creative Commons Attribution License, which permits use, distribution and reproduction in any medium, provided the original work is properly cited.

© 2026 The Author(s). *Journal of Cosmetic Dermatology* published by Wiley Periodicals LLC.

line of defense for cutaneous homeostasis [2]. Sebum consists mainly of triglycerides and free fatty acids (~57%), wax esters (26%), squalene (12%), and cholesterol (2%). Under physiological conditions, sebum lubricates both the skin and hair shafts, while its metabolic byproducts—particularly free fatty acids—contribute to maintaining the mildly acidic pH of the skin surface, which is crucial for antimicrobial defense [3, 4].

In adults, the normal sebum secretion rate is approximately 1 mg/10 cm^2/3 h; rates exceeding this threshold result in oily skin [5]. Hypersecretion of sebum, or seborrhea, leads to oily skin, enlarged pores, and increased adhesion of environmental pollutants and is closely associated with the pathogenesis of multiple skin disorders [6]. The accumulation of sebum obstructs pilosebaceous ducts, fostering an anaerobic environment that facilitates the proliferation of microorganisms, including *Cutibacterium acnes*. This stimulates inflammatory responses, leading to the development of comedones, acne vulgaris, and seborrheic dermatitis [7–9].

These conditions are most common among adolescents aged 10–19 years, whose endocrine fluctuations, especially increased androgen levels, markedly enhance sebaceous gland activity [10–12]. The interplay of dietary and lifestyle factors with this hyperactivity significantly increases the prevalence of sebum-related skin problems, adversely affecting mental health and social well-being [13–15]. Therefore, the development of safe and effective methods to regulate sebum secretion without disrupting physiological development holds considerable clinical and commercial importance.

Recently, bioactive compounds derived from natural plants have garnered significant interest in dermatological and cosmetic research due to their abundant availability, diverse biological activities, and acceptable safety profiles. The functional components of plant extracts include polyphenols (flavonoids and phenolic acids), polysaccharides, terpenoids, alkaloids, and organic acids [16, 17]. Flavonoids, including anthocyanins and resveratrol, exhibit potent antioxidant and anti-inflammatory effects, alongside antiaging, whitening, and microcirculation-enhancing activities by modulating angiogenesis and inhibiting matrix metalloproteinase (MMP) activity [18, 19]. Phenolic acids, including tea polyphenols, inhibit tyrosinase activity, stimulate collagen and elastin synthesis, and provide antimicrobial and photoprotective benefits [20–22]. Plant polysaccharides, including those sourced from peach gum and *Astragalus*, have demonstrated efficacy in mitigating ultraviolet B-induced photoaging by regulating oxidative stress and inflammatory pathways, as well as in facilitating wound healing through increased collagen deposition and angiogenesis [23–26]. In addition to its anti-inflammatory, antiaging, and whitening effects, Youyun Liu et al. [27] also found that *Ludwigia adscendens* (L.) Hara extract can regulate the PPAR γ/LXR α/SREBP1 pathway and inhibit the production of excessive sebum. Polyphenols in green tea and apples inhibit targets such as SREBP1 to reduce sebum to varying degrees [28, 29]. Polysaccharide from Prinsepia utilis Royle was found to enhance skin barrier integrity by promoting keratinocyte differentiation, lipid metabolism, and tight junctions [30]. Lu Cheng et al. [31] also found in clinical research that *Lotus corniculatus* seed extract immediately and permanently reduced the sebum content and area of oily skin. These findings show that plants and the ingredients contained in plants have a certain effect on sebum secretion, which is a valuable reservoir for novel skin health-promoting ingredients.

Litchi (*Litchi chinensis Sonn.*), a subtropical evergreen fruit tree belonging to the Sapindaceae family, originates from Southern China and is now cultivated widely in tropical and subtropical regions globally [32, 33]. The pulp is the primary edible component, although large quantities of byproducts, including pericarp (peel) and seeds, are frequently discarded [34, 35]. Recent phytochemical studies have demonstrated that *litchi* byproducts, especially the pericarp, are abundant in bioactive compounds, including polysaccharides, polyphenols, flavonoids, and saponins. For instance, Gao et al. reported that *litchi* pericarp polysaccharides exhibit significant in vitro antioxidant activity [36]. Phenolic compounds, including proanthocyanidins and epicatechin, possess potent antioxidant, antiaging, and whitening effects through free radical scavenging, metal ion chelation, and inhibition of collagenase and tyrosinase [37–40]. Furthermore, flavonoids from *litchi* leaf extract exhibit photoprotective activity by absorbing ultraviolet radiation and alleviating oxidative stress and DNA damage [41, 42].

Despite increased evidence supporting the antioxidant, antiaging, and whitening properties of *litchi* extracts, their potential role in modulating sebaceous gland activity and reducing excessive sebum secretion remains unexplored. This knowledge gap indicates a need for systematic investigation. Sebum hypersecretion is a key pathogenic factor implicated in various skin disorders. Given the well-documented anti-inflammatory and antioxidant properties of litchi-derived bioactive compounds, this study aimed to evaluate the regulatory effects of *litchi* extracts on sebum secretion and clarify the associated molecular mechanisms. Specifically, we prepared fraction-enriched samples from crude *litchi* extracts using a murine model of seborrheic dermatitis to determine the most effective fraction for restoring skin oil–water balance and mitigating inflammation in vivo. To further explore the underlying biological mechanisms, we conducted transcriptomic profiling and fluorescence intensity test of oil secretion using immortalized human sebocytes (SZ95) as an in vitro model. This approach will facilitate the identification of key signaling pathways and molecular targets involved in the regulation of sebum synthesis and secretion. Collectively, the findings from this study are expected to provide a scientific basis for developing *litchi* extract as a novel sebum-regulating ingredient for dermatological and cosmetic applications.

2 | Materials and Methods

2.1 | *Litchi chinensis* Extraction Technology

Litchi chinensis procured from Zengcheng, Guangzhou, Guangdong Province, was crushed into small fragments and extracted using 30% ethanol under reduced pressure and ultrasonic reflux for 1.5 h. The resultant concentrated solution was extracted to yield 100% crude drug (ultrasonic reflux extraction equipment, Shanghai Haochu Machinery Equipment Co. Ltd., China). The mixture was filtered with a 0.45 μm filter membrane until it was clear, and the filtrate was concentrated under

reduced pressure to obtain 200% crude drug (rotary evaporator, Xi'an Yuhui Experimental Instrument Co. Ltd., China) and molecularly imprinted polymer. The sample loading ratio was converted into medicinal material mass: molecular imprinted polymer mass = 4:3, and the sample loading permeate was ultrafiltered with a 10 000 Da ultrafiltration membrane. The permeate was concentrated and depressurized to a total phenol content of 0.6%, and butanediol (Crasua Chemical Inc., China) and glycerol (SWAN BRAND, China) were added to formulate a solution comprising 45% butanediol and 15% glycerol, resulting in *litchi* extract 1 (ZY1). The retentate was concentrated and depressurized until the total sugar content reached 0.2%. Subsequently, we added 0.5% of p-hydroxyacetophenone (Nantong Dezhixin Fragrance Co. Ltd., China) and 0.6% of 1,2-hexanediol (Xincheng Materials Co. Ltd., Japan) to obtain *litchi* extract 3 (ZY3). The molecularly imprinted material used for extract adsorption was washed with pure water (twice the mass of the molecularly imprinted polymer) and eluted with 95% ethanol (four times the molecularly imprinted polymer mass). The eluate was concentrated to 0.6% of total flavonoids, and a solution containing 45% butanediol and 15% glycerol was prepared by adding butanediol and glycerol. The permeate was ultrafiltered through an ultrafiltration membrane of 10 000 Da and desalted with a nanofiltration membrane of 150–300 Da until the conductivity was < 100 μS/cm, yielding *litchi* extract 2 (ZY2). The molecularly imprinted material used was synthesized as described in Example 2 in Chinese patent CN202411497901.6.

ZY2 was qualitatively analyzed by LC-2050C liquid chromatograph (Shimadzu Corporation, Japan). Inertsil ODS-HL C18 column (250 * 4.6 mm, 5 μm) was used, and gradient elution method was adopted, with the flow rate of 1.0 mL/min. The mobile phase used to detect the main components is composed of 0.1% phosphoric acid (A, Shanghai Aladdin Biochemical Technology Co. Ltd.) and acetonitrile (B, Shanghai Macklin Biochemical Technology Co. Ltd.). The procedures of gradient elution of rutin/naringin/quercitrin/phloridzin are as follows: 18%–22% (B) for 0–3 min and 22% (B) for 3–30 min; the procedure of gradient elution of isoquercitrin/luteolin is 12%–21% (B) for 0–25 min, 21%–30% (B) for 25–35 min and 30%–12% (B) for 35–40 min. The column temperature is set to 40°C. The injection volume is set to 20 μL. All samples were filtered through 0.45 μm disposable filter paper. Accurately weigh the reference standards of rutin, quercitrin, luteoloside, naringin, isoquercitrin and phloridzin (Manchester Biotechnology Co. Ltd., China), and dissolve them with methanol to prepare the reference solution.

2.2 | Animal Experiment

2.2.1 | Modeling of Seborrheic Dermatitis in Mice

All animal procedures are carried out in accordance with relevant guidelines and regulations. Male ICR mice (weighing 20–25 g) were obtained from Shanghai Jiesijie Experimental Animal Co. Ltd. The animals were housed under standard laboratory conditions with a natural temperature of 25°C–32°C, humidity of 40%–60%, and a normal light/dark cycle without special control. The mice were allowed to acclimatize for 3–7 days before the experiment commenced. The mice were randomly divided into six groups (BC: blank control, NC: model control, PC: positive control, ZY1: litchi extract 1, ZY2: litchi extract 2, and ZY3: litchi extract 3), with six mice in each group. After 5 days of adaptive feeding, a 2 × 2 cm area on the dorsal skin of each mouse was shaved. The mice in the BC group received normal maintenance feed, and those in the other groups were fed with modeling feed (2.3 g fish oil and 46 g linoleic acid were added to every 100 g mouse feed, Jiangsu Medisen Biomedicine co. Ltd.) for 4 weeks. Additionally, a mixture of passive fish oil (Nanjing Dulai Biology Technology Co. Ltd.)/linoleic acid (Shanghai Macklin Biochemical Co. Ltd.) (1:20) in a 1:20 ratio was administered via oral gavage during the first 15 days of the experiment. Besides, 0.4 mL of the mixture was administered twice daily (morning and evening) from days 1 to 10, and from days 11 to 15, the dosage was reduced to 0.3 mL twice daily (morning and evening). Simultaneously, topical drug smearing treatment was performed as part of the treatment regimen.

On day 1, skin inflammation was induced using 2,4-dinitrochlorobenzene (DNCB, TCI (Shanghai) Development Co. Ltd.). On day 1 before the experiment, the abdominal and dorsal regions of the mice were depilated. To induce sensitization, 50 μL of a 5% DNCB solution in ethanol was evenly applied to the depilated area of the lower abdomen at 9:00 a.m. on both days 1 and 2. On day 6 of the experiment, 25 μL of 1% DNCB ethanol solution was applied to the back depilation area (2 × 2 cm) located 1 cm above the base of the tail on the dorsal side of each mouse. This stimulation was performed once every 3 days, for six applications, all administered at 9:00 am. Preventive treatments were initiated concurrently with the sensitization phase. BC and NC groups were smeared with 0.2 mL of pure water daily, while the PC group was smeared with 0.1 g of sulfur ointment (He'nan Daxin Drug Co. Ltd.) every 3 days. ZY1, ZY2, and ZY3 groups were smeared with 0.2 mL of 1% solution daily, on the affected 2 × 2 cm area, continuing until the end of the stimulation period. After feeding for 4 weeks, each group of mice was weighed again. At the end of the experiment, the skin condition of mice in each group was visually assessed and documented through photographic records.

2.2.2 | Evaluation of Skin Lesions and Determination of Skin Water and Oil Content

The clinical appearance score was utilized to evaluate the appearance of different groups of mice. The region to be observed included the nape of the neck (the area from the top of the head to the tail), the ear root and mouth region, the healing site, and a section of the limb's root with less hair. The appearance score was determined based on the primary manifestations of three pathological symptoms of seborrheic dermatitis (skin redness, scaling, and depilation). The scoring system for each lesion was 0–3: 0 indicates no obvious symptoms; 1 point indicates mild lesions; 2 points indicate moderate lesions; and 3 points signify severe lesions. The total evaluation score was the sum of the symptom scores from the three lesions.

On the last day of the experiment, skin moisture and oil content were measured using a skin moisture tester (MoistureMeter SC, MSC1473) and a sebum tester (SebumScale, SSC1110). The ratio of water content to oil content (water content/oil content)

was calculated to evaluate the level of water and oil content in mouse skin.

2.2.3 | Hematoxylin and Eosin (H&E) Staining and Oil Red Staining

Mouse skin tissue samples were fixed with universal tissue fixative (Servicebio, G1101), dehydrated, paraffin-embedded, sectioned, dewaxed, stained with H&E (Servicebio, G1076), dehydrated, and sealed. After the frozen sections were fixed, they were stained with Oil Red dye solution and hematoxylin, and the staining was examined microscopically and sealed. An optical microscope (NIKON ECLIPSE E100, Japan, magnification of 20× and 200×) was utilized to assess and analyze the inflammation level of the epidermis and dermis, and the positive proportion area of fat cells in each group was evaluated using Aipathwell software (a digital pathological image analysis software based on artificial intelligence learning introduced by Servicebio Company).

2.3 | Sebaceous Gland Cell Transcriptomics

2.3.1 | Cell Activity Test and RNA Extraction, Library Preparation, and High-Throughput Sequencing

Human sebaceous gland cell SZ95 (supplied by Yunse Bioscience Co. Ltd., Shanghai) was cultured in a cell incubator (Thermo Fisher Scientific) at 37°C with 5% CO_2. The cells were incubated in a high-glucose Dulbecco's modified Eagle medium (DMEM) supplemented with 10% heat-inactivated fetal bovine serum (FBS) (Thermo Fisher Scientific, Waltham, MA, USA) and a 100 U/mL penicillin/streptomycin mixture (Thermo Fisher Scientific). The cell relative activity of the ZY2 was tested using the MTT (Thermo Fisher Scientific) method, with the following formula:

$$\text{Cell relative activity} = \left(\frac{OD_{TA}}{OD_B}\right) \times 100\%$$

, where OD_{TA} represents the third average of the optical density of the tested sample group, and OD_B denotes the third average of the optical density of the blank control group.

The SZ95 cell suspension was inoculated on 6-well cell culture plates and incubated for 24 h. After incubation, the plates were removed and washed with PBS for 2–3 times. The cells were subsequently divided into a blank control group (B, culture medium), a negative control group [NC, linoleic acid (Thermo Fisher Scientific) + culture medium], and a sample group to be tested (Lychee, ZY2 + linoleic acid + culture medium) and incubated for 24 h (three biological replicates for each treatment). Following treatment, the 6-well plates were again washed with PBS for 2–3 times. Total RNA was extracted using an RNA extraction kit (QIAGEN GmbH, Germany), and the PrimeScript RT Master Mix kit (Takara Bio Inc., Beijing), RT-PCR detection kit (Takara Bio Inc., Beijing), and RNA quantitative kit (Thermo Fisher Scientific) were used to extract RNA and detect its purity and concentration. The DNA quantitative kit (Thermo Fisher Scientific) and mRNA enrichment kit (Illumina, USA) were used to enrich mRNA fragments and synthesize cDNA. The RNA library building kit (Illumina, USA) was utilized to prepare the RNA-seq library. The obtained library was mixed, and high-throughput sequencing was performed with a sequencer (Illumina, USA).

2.3.2 | RNA Sequencing (RNA-Seq)

Use FastQC (v0.10.1) to evaluate the quality of raw sequencing data, and use Fastp (v0.24.1) to remove adapter sequences and low-quality bases to obtain high-quality Clean Reads. Align Clean Reads to the reference genome (GRCh38/hg38) using Hisat2 (v2.2.1). Then, using EigenCounts (v2.0.1) to compare and count the reads to the explicit subregion, the original expression matrix is generated. Based on the above counting matrix, DESeq2 (v1.26.0) R package was used for differential expression gene analysis. DESeq2 uses a negative binomial generalized linear model to fit the data and conducts significance hypothesis testing using Wald test. Quantitative analysis of gene expression levels was performed using Feature Counts software, and differentially expressed genes (DEGs) were screened using DESeq2 software according to the criteria of Padj (FDR) < 0.05 and $|\log_2 \text{FoldChange}| \geqq 0$. Subsequently, gene ontology (GO) and Kyoto encyclopedia of genes and genomes (KEGG) analyses were conducted on DEGs using clusterProfiler (v3.18.0) to identify the key enriched biological functions and metabolic pathways. The DEGs in the significantly enriched items were further examined to determine the key core genes [43]. The protein–protein interaction (PPI) network was constructed using Cytoscape (3.10.1). The specific transcriptome analysis was conducted by YUNSEBIOSCIENCE (Shanghai) CO. LTD.

2.4 | Fluorescence Intensity Detection of Cellular Oil Secretion

Inoculate the SZ95 suspension of human sebaceous gland cells into a 96 well cell culture plate and culture for 24 h. Take out a 96 well plate and divide it into four groups: blank control group (BC, high glucose DMEM medium), negative control group (NC, linoleic acid (Thermo Fisher Scientific) + high glucose DMEM medium), positive control group (PC, linoleic acid + isotretinoin (Shanghai Yuanye Bio Technology Co. Ltd) + high glucose DMEM medium), and test sample group (0.1% ZY2 + linoleic acid + high glucose DMEM medium). Add corresponding substances and culture for 24 h (three biological replicates per treatment). After cultivation, wash with PBS and add paraformaldehyde (Biosharp), then let it stand at room temperature. Add Triton X-100 (Sigma) and let it stand at room temperature. Add Nile Red working solution (Shanghai Aladdin Biochemical Technology Co. Ltd.) and incubate at room temperature in the dark. Take photos under a fluorescence microscope (Olympus Corporation) in the dark. Use ImageJ software to analyze the fluorescence intensity of the collected photos. The inhibition rate of oil secretion is calculated using the following formula:

$$\text{Oil secretion inhibition rate} = \left(1 - \frac{B - A}{C - A}\right) \times 100\%$$

A: fluorescence intensity of BC; *B*: fluorescence intensity of test sample group; *C*: fluorescence intensity of NC.

2.5 | Data Processing and Analysis

Excel software was utilized for data analysis. The data of each group are expressed as mean ± standard deviation ($\overline{X} \pm S$). Comparison between groups was conducted using Student's *t*-test. A $p < 0.05$ was considered statistically significant compared with the model group.

3 | Results

3.1 | Effects of Litchi Extracts From Three Different Extraction Processes on the Skin Condition of Mice

Initially, three different *litchi* extracts were obtained: *litchi* extract 1 (ZY1) with 0.6% total polyphenols, *litchi* extract 2 (ZY2) with 0.6% total flavonoids, and *litchi* extract 3 (ZY3) with 0.2% total polysaccharides, based on three different technologies. To investigate the therapeutic efficacy of litchi extract obtained by three different techniques on seborrheic dermatitis and its capacity for oil–water balance, we created a model on the skin of mice and smeared the corresponding *litchi* extract for observation. After a 30-day experiment, we assessed the severity of skin lesions in mice in each group. Figure 1A depicts that the skin lesions of mice in the NC group exhibited a high score. However, after giving different samples, the skin lesions of mice in each treatment group were significantly improved compared with those in the NC group, whereas the severity of skin lesions in the ZY3 group did not significantly differ from that in the NC group. The water and oil content of mice skin in each group was measured, and the ratio of water content to oil content (water content/oil content) was calculated to evaluate the level of water and oil content of mice skin. Figure 1B indicates that the water–oil ratio of mice in the NC group decreased significantly compared to that of mice in the BC group, indicating severe damage to the water–oil balance. After the treatment of each sample, the water–oil ratio of the mice's skin increased to varying degrees, with ZY2 demonstrating a significant effect. At the end of the experiment, the skin state of each group of mice was assessed, and the skin appearance state was recorded through photography. The results are illustrated in Figure 1C,D. The skin of mice in each group exhibited significant damage and creasing. After the other groups were treated with drugs, the skin was significantly improved compared to the NC group.

3.2 | Effects of Litchi Extracts From Three Different Extraction Processes on Skin Histological Changes

H&E staining and ORO staining were utilized to observe the structural damage of three *litchi* extracts to the skin of mice. As shown in Figure 2A, the epidermis of group BC's skin tissue is intact, with a clear structure and visible stratum corneum. The collagen fibers in the dermis layer are arranged neatly, and the number of hair follicles and sebaceous glands in the skin is abundant. The NC group showed mild hyperkeratosis of the local epidermis, thickening of the granular layer, and spinous layer. A small amount of cytoplasmic vacuolization was observed in the epidermal spinous layer, and a small amount of connective tissue hyperplasia was observed in the superficial dermis layer. Compared with the NC group, the PC group, ZY1 group, and ZY2 group were able to alleviate the above situation. However, in the ZY3 group, small areas of necrosis were observed in the epidermis of the skin tissue, with fragmented or condensed nuclei, and a small amount of incomplete keratinization was observed in the necrotic stratum corneum. Hyperkeratosis of the epidermal stratum corneum can be seen in multiple places, with a small amount of proliferation of spinous cells, elongation of skin processes, and a small amount of connective tissue proliferation in the superficial dermis layer. The ORO staining (Figure 2B), analyzed using Aipathwell software, revealed the lipid-positive area ratios (%) of groups BC, NC, PC, ZY1, ZY2, and ZY3 were 6.9, 18, 15.5, 12.6, 6.6, and 19, respectively. Comprehensive results 3.1 and 3.2 indicate that the ZY2 treatment group significantly improved inflammatory symptoms and contributed to the water–oil balance of skin in mice with mixed contact dermatitis.

3.3 | Analysis of Flavonoids in ZY2

We used HPLC to analyze the flavonoid composition of ZY2 with a total flavonoid content of 0.6%. As shown in Figure 3, the flavonoids of ZY2 mainly include rutin, quercitrin, luteoloside, naringin, isoquercitrin, and phloridzin.

3.4 | Transcriptome Sequencing Data Statistics and Quality Evaluation

Before the transcription of ZY2 samples, the SZ95 cell activity was tested using the MTT method. The results revealed that when the concentration of ZY2 samples was ≤0.1%, the cell activity was more than 90%, which could be used in subsequent experiments. Consequently, 0.1% was selected as the test concentration of subsequent experiments. The mRNA expression of different treatment groups was studied, including three groups, three biological repeats in each group, and a total of nine samples, based on Illumina sequencing [44]. We sequenced 399 903 337 original data, and subsequently mapped the measured data to the reference genome, and 394 444 067 quality-controlled data were obtained. The mapping rate of sequencing sequences (total_map) was higher than 97% on the premise that the annotation of the reference genome was complete and there was no pollution in related experiments. Moreover, Q20 and Q30 were more than 96%. It is generally believed that Q20 is more than 85% and Q30 is more than 80%, which can meet the quality requirements of sequencing, and the GC content (approximately 50%) and base mass distribution were excellent (Table 1). The data and quality of this sequencing have reached the requirements of subsequent analysis.

3.5 | Screening of DEGs

DEGs were screened according to the criteria of Padj (FDR) < 0.05 and $|\log_2 (\text{Fold Change})| \geqq 0$, and the results are illustrated in

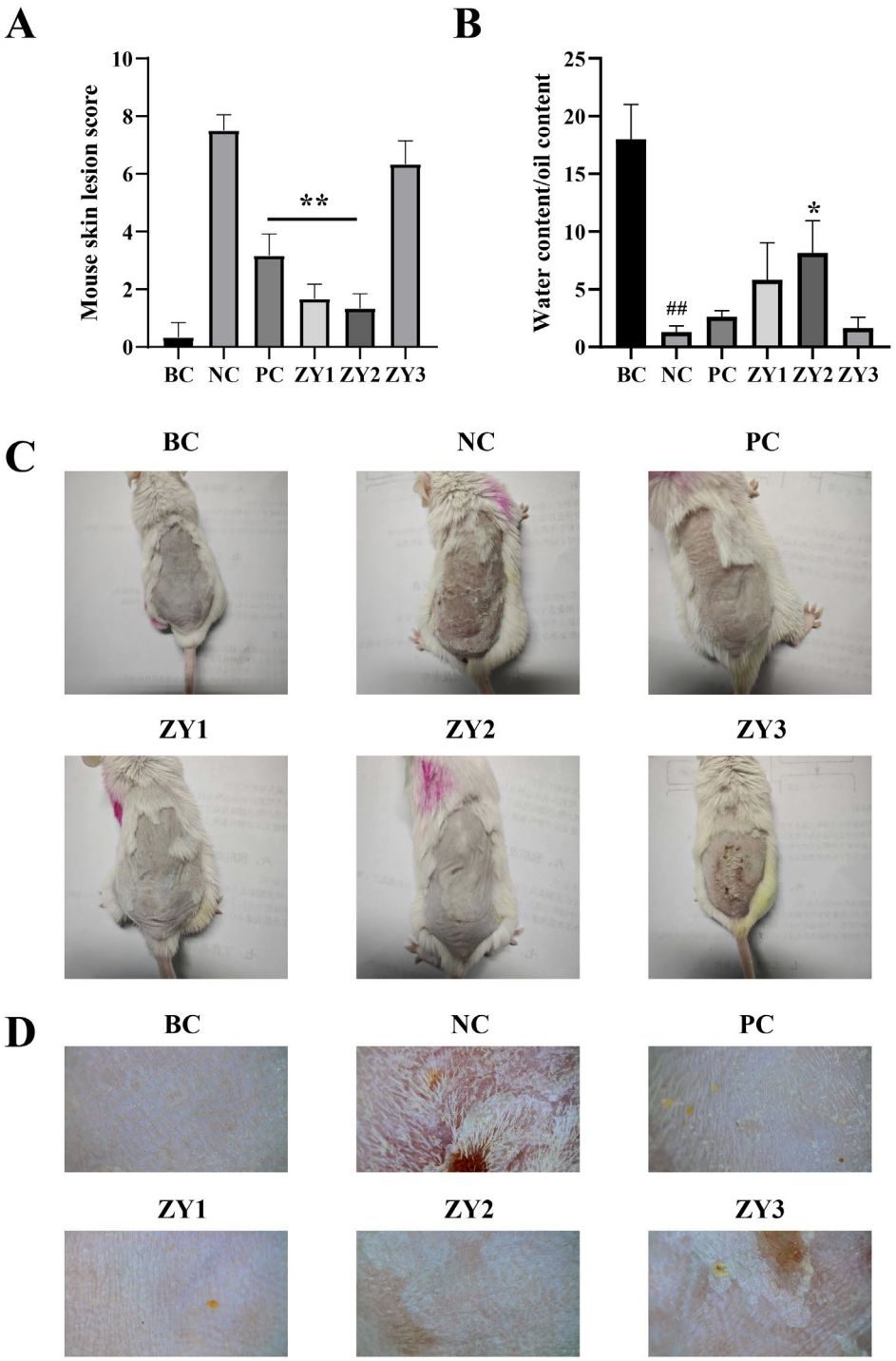


FIGURE 1 | Effects of litchi extracts from three different extraction processes on the skin condition of mice ($n = 6$). (A) Scoring the degree of skin lesions in mice. $^{**}p < 0.01$ vs the NC group. (B) Water–oil content ratio of mouse skin. $^{\#\#}p < 0.01$ vs the BC group. $^{*}p < 0.05$ vs the NC group. (C, D) Apparent state of mouse skin, and (D) the state observed under a microscope, with a magnification of 10×. All experiments were carried out in biological replicates.

Figure 4. Compared with the blank control (B group), 6740 DEGs were screened from the negative control (NC group), including 3262 upregulated genes and 3478 downregulated genes (Figure 4A). Compared with the negative control (NC group), 2241 DEGs were screened in the sample group (Lychee group), including 832 upregulated genes and 1409 downregulated genes (Figure 4B).

3.6 | Functional Enrichment Analysis of NC Versus B Differential Genes

Compared to group B, 3262 DEGs were upregulated and 3478 DEGs were downregulated in the NC group ($p < 0.05$). GO and KEGG function enrichment analyses were conducted on the DEGs that met the above conditions. The upregulated gene GO

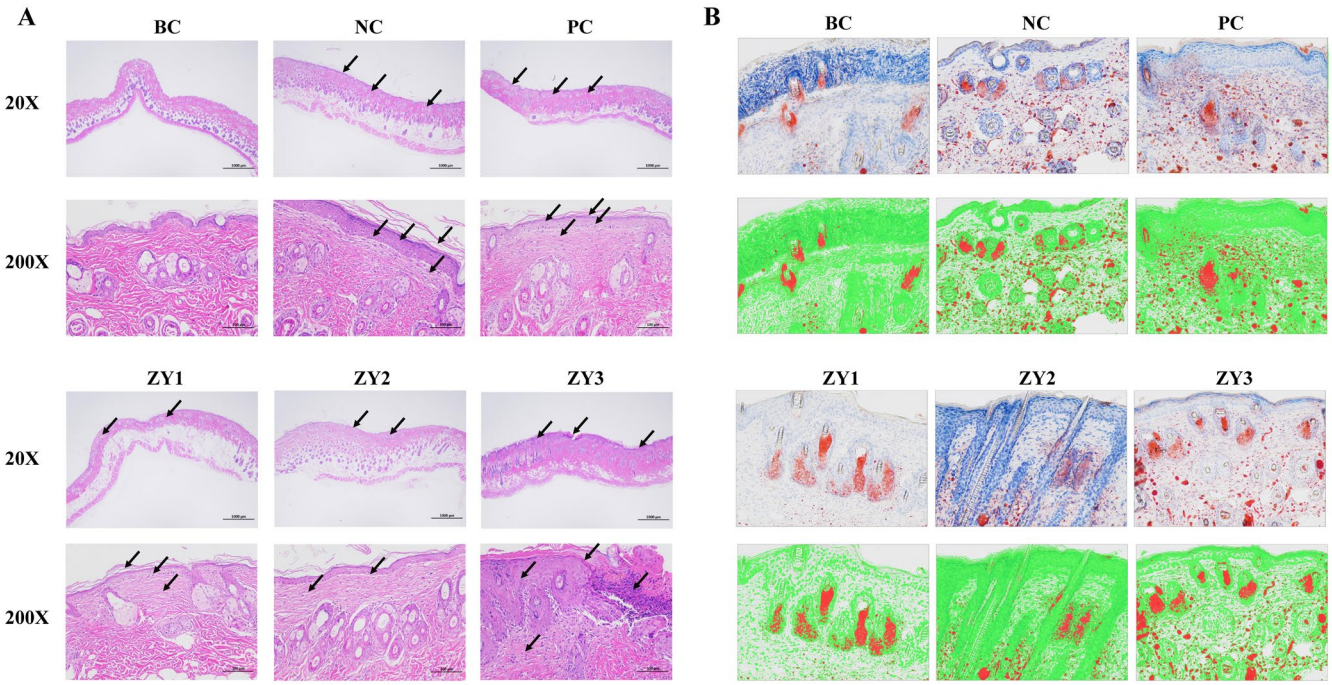


FIGURE 2 | Effects of litchi extracts from three different extraction processes on the histological changes of skin ($n = 6$). (A) The results of H&E staining of mouse skin tissue revealed that the microscope magnification was 20× and 200×. (B) The results of ORO staining of mouse skin tissue and the fluorescent green chart were obtained by using Aipathwell software. All experiments were carried out in biological replicates.

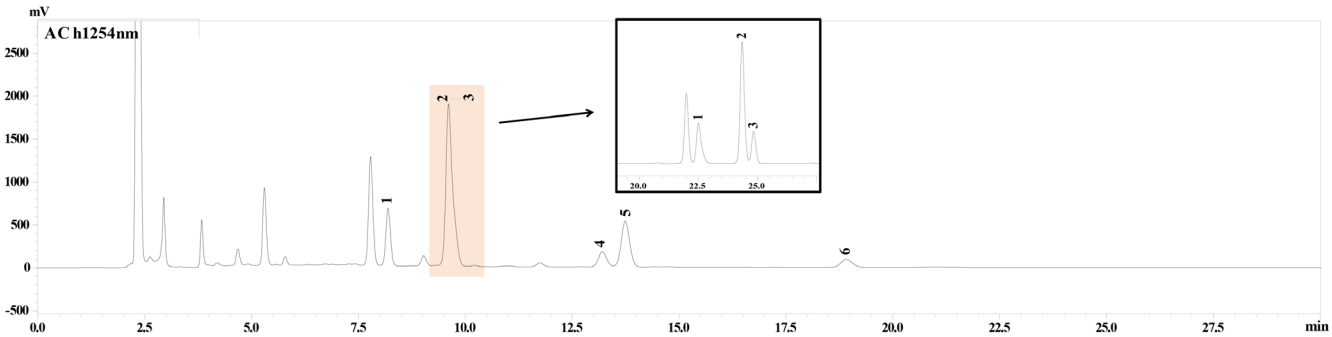


FIGURE 3 | HPLC diagram of ZY2 flavonoids. Numbers 1, 2, 3, 4, 5, and 6 in the figure represent rutin, isoquercitrin, luteoloside, naringin, quercitrin, and phloridzin respectively.

TABLE 1 | Summary of the raw data obtained by RNA sequencing.

Sample	Raw reads	Clean reads	Total_map	Q20	Q30	GC_pet
B_1	47 190 012	46 912 362	46 003 526 (98.06%)	99.02	97.02	50.47
B_2	40 750 088	40 304 150	39 507 082 (98.02%)	99.00	97.04	50.64
B_3	41 275 814	40 794 790	39 963 327 (97.96%)	98.95	96.88	50.64
NC_1	46 396 726	45 076 808	44 085 418 (97.8%)	98.93	96.95	50.81
NC_2	42 756 894	41 896 948	40 967 094 (97.78%)	98.91	96.89	50.70
NC_3	46 599 386	45 642 706	44 686 706 (97.91%)	99.00	97.09	50.73
Lychee_1	45 592 264	45 077 938	44 094 491 (97.82%)	98.99	97.02	50.61
Lychee_2	45 362 735	45 362 735	44 072 566 (97.16%)	98.95	97.03	49.72
Lychee_3	44 176 832	43 375 630	42 121 141 (97.11%)	98.96	97.05	49.71

Note: Raw reads: the number of reads in the original data; Clean reads: the number of reads after quality control filtering of the original data; Total_map: the number and percentage of reads matched to the genome; Q20: data ratio with base sequencing error rate < 1%: Q30: data ratio with base sequencing error rate < 0.1%. Abbreviation: GC _ PCT, percentage of G and C in clean reads.

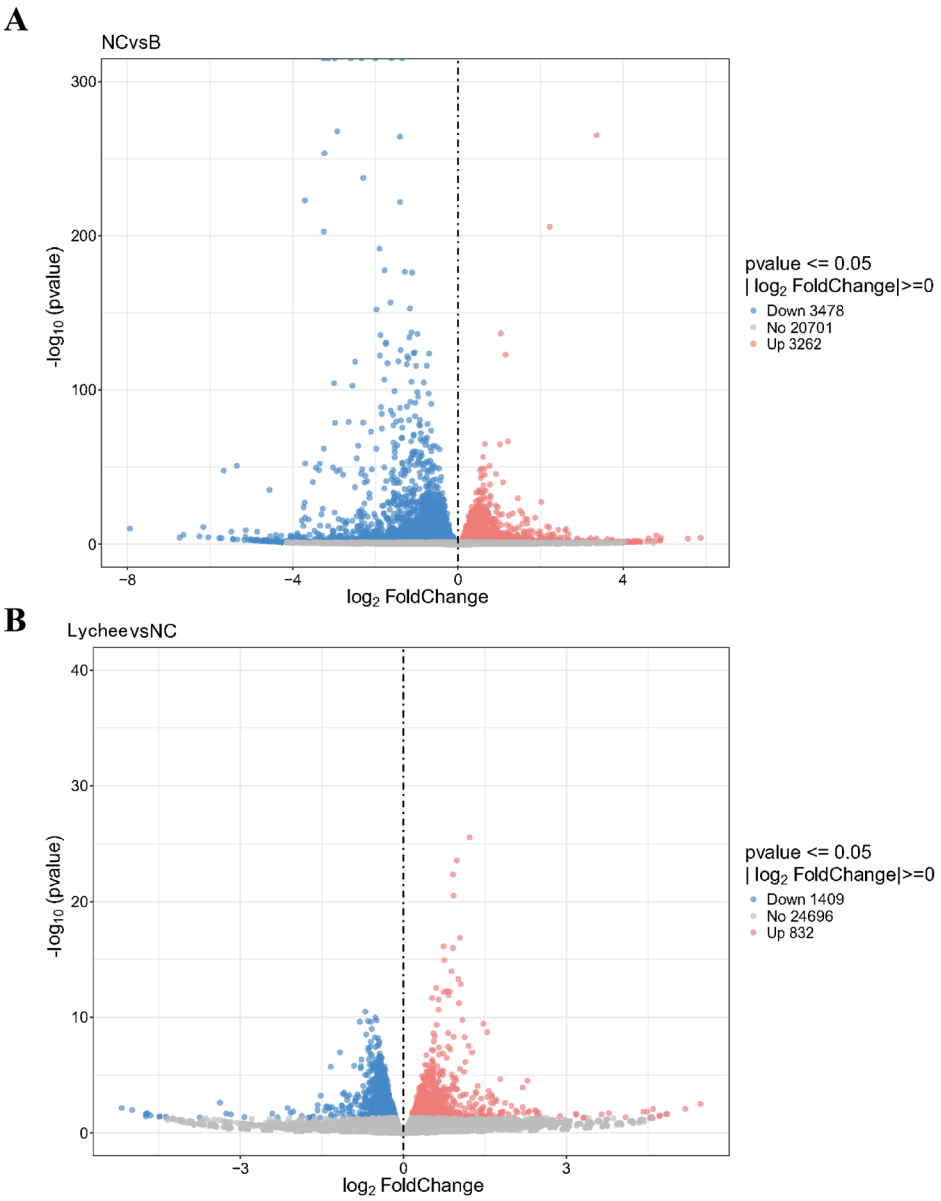


FIGURE 4 | Volcano map of DEGs. (A) Volcano map comparing DEGs between the blank control (B group) and the negative control (NC group). (B) Volcano map comparing DEGs between the negative control (NC group) and the sample group (Lychee group). The black dotted line represents the value line of differential gene screening criteria; each point in the graph represents a gene; red indicates significantly upregulated DEGs; blue indicates significantly downregulated DEGs; gray indicates genes with no significant DEGs. In the figure, the abscissa represents the change of gene expression multiple ($\log_2$(Fold Change)) in the treatment and control groups, and the ordinate represents the significant level of gene expression difference ($-\log_{10}$(p value)) in treatment and control groups. For this result, three independent biological replicates were performed.

function enrichment analysis revealed 738 enrichment items, and the KEGG pathway enrichment analysis revealed 328 signal pathways. Conversely, the downregulated gene GO function enrichment analysis revealed 754 enrichment items, and the KEGG pathway enrichment analysis revealed 334 signal pathways. Using the enrichment factor comparison, p value and Med-Explorer database, 20 biological functions and signal pathways exhibiting the highest correlation were selected for analysis of upregulated genes via GO and KEGG (Figure 5A), whereas 20 biological functions and 10 signal pathways with the highest correlation were selected for analysis of downregulated genes via GO and KEGG (Figure 5B). The examination of biological function analysis of GO revealed that the upregulated genes induced by linoleic acid primarily pertain to fatty acid and triglyceride synthesis, whereas the downregulated gene expression predominantly influences protein kinase activity, ATP metabolism and fatty acid metabolism. KEGG signal pathway analysis revealed that the genes upregulated and downregulated by linoleic acid predominantly pertain to lipid metabolism, growth, differentiation, and energy metabolism, with the clustering of upregulated genes enriching more signal pathways associated with fat anabolism compared to downregulated genes.

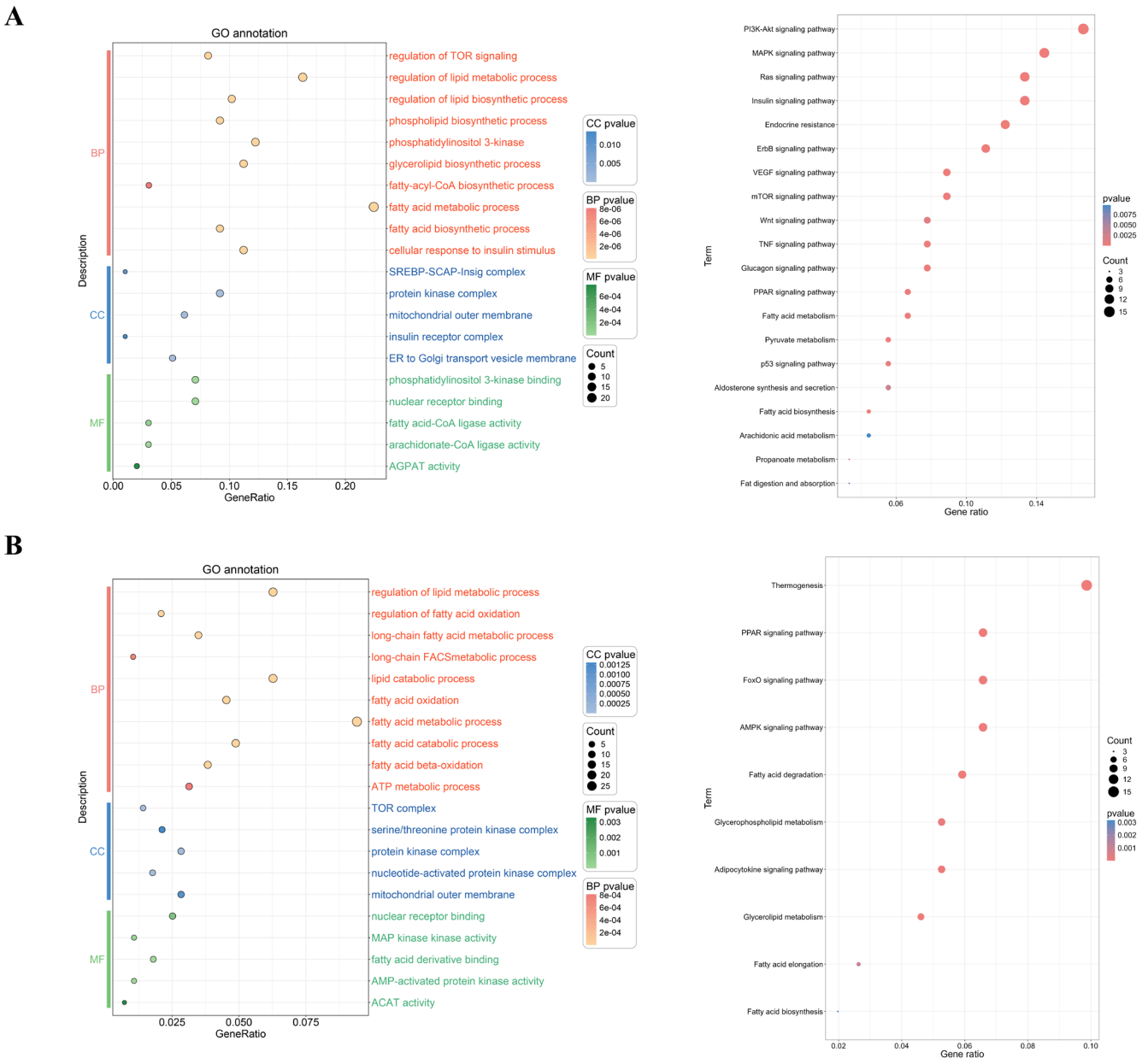


FIGURE 5 | GO and KEGG analyses of NC versus B differential genes. (A) Upregulating GO and KEGG of genes. (B) Downregulating GO and KEGG of genes. For this result, three independent biological replicates were performed.

3.7 | Functional Enrichment Analysis of Lychee Versus NC Differential Genes

Compared to the NC group, 832 DEGs were upregulated and 1409 DEGs were downregulated in the Lychee group ($p < 0.05$). GO and KEGG function enrichment analyses were conducted on the DEGs that met the above conditions. GO function enrichment analysis of upregulated genes yielded 531 enrichment items, whereas KEGG pathway enrichment analysis revealed 306 signaling pathways. A GO function enrichment study of downregulated genes revealed 646 enrichment items, whereas KEGG pathway enrichment analysis revealed 310 signaling pathways. Utilizing the enrichment factor comparison, *p* value, and Med-Explorer database, 20 biological functions and 10 signal pathways exhibiting the highest correlation were identified for analysis of upregulated genes via GO and KEGG (Figure 6A), while 20 biological functions and signal pathways with the highest correlation were selected for analysis of downregulated genes via GO and KEGG (Figure 6B). The biological function analysis of GO revealed that the upregulated genes resulting from the inclusion of the Lychee sample predominantly affected protein kinases and other regulatory pathways, whereas the downregulated genes primarily involved lipid metabolism and oxidation in human sebaceous cells. KEGG signal pathway analysis revealed that the upregulated genes in lychee primarily pertain to cell growth, differentiation, signal transduction, and immunological control, whereas the downregulated genes primarily relate to lipid metabolism, energy balance, and cell signal transduction.

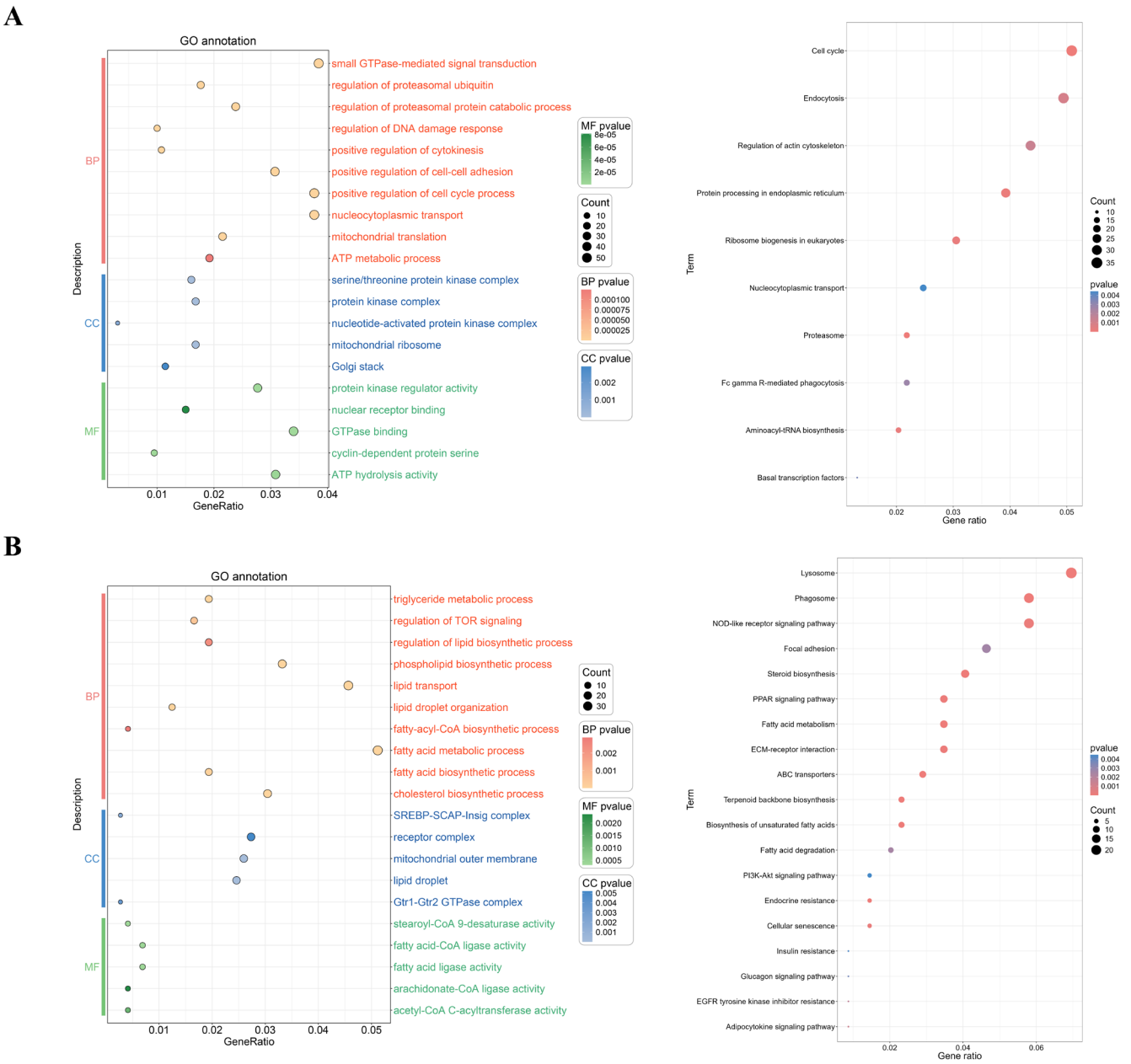


FIGURE 6 | GO and KEGG analyses of Lychee versus NC differential genes. (A) Upregulating GO and KEGG of genes. (B) Downregulating GO and KEGG of genes. For this result, three independent biological replicates were performed.

3.8 | Statistics and Analysis of Key Differential Genes

DEGs of NC versus B and the oil control target from the Med-Explorer database were mapped and intersected, resulting in the identification of 103 target genes. DEGs of Lychee versus NC were mapped and intersected with the list of oil control targets in the Med-Explorer database, resulting in the identification of 112 target genes. The target genes from the three groups were mapped and intersected, resulting in the identification of 36 target genes associated with lipid metabolism. The gene expression level of these 36 targets is illustrated in a heatmap (Figure 7A). In Figure 7A, different colors indicate the $\log_2$FoldChange of gene expression, with blue denoting downregulation of gene expression and red signifying upregulation of gene expression. Compared with the blank control group, linoleic acid significantly upregulated some genes and downregulated others. Post-intervention, the expression levels of these genes can be effectively restored and sustained. Compared with the NC group, 29 genes were significantly downregulated, and 7 genes were significantly upregulated.

In the subsequent analysis of the results after sample intervention, we combined the gene expression data after sample intervention with the function enrichment analysis results of differential genes from results 3.5 and 3.6 and systematically summarized the DEGs related to skin oil secretion and their corresponding signal pathways through the PPI network (Figure 7B). These DEGs were primarily concentrated in the following pathways: fatty acid metabolism, fatty acid degradation, insulin resistance, PI3K-Akt signaling pathway, AMPK

signaling pathway, and glyceride metabolism. The enrichment analysis of these pathways revealed that sample intervention may significantly influence skin oil secretion by regulating these critical signal pathways.

We examined the enrichment pathways of DEGs and their upstream and downstream relationships, constructing a relevant signal pathway analysis diagram of skin lipid metabolism. The diagram illustrates the interaction between upstream and

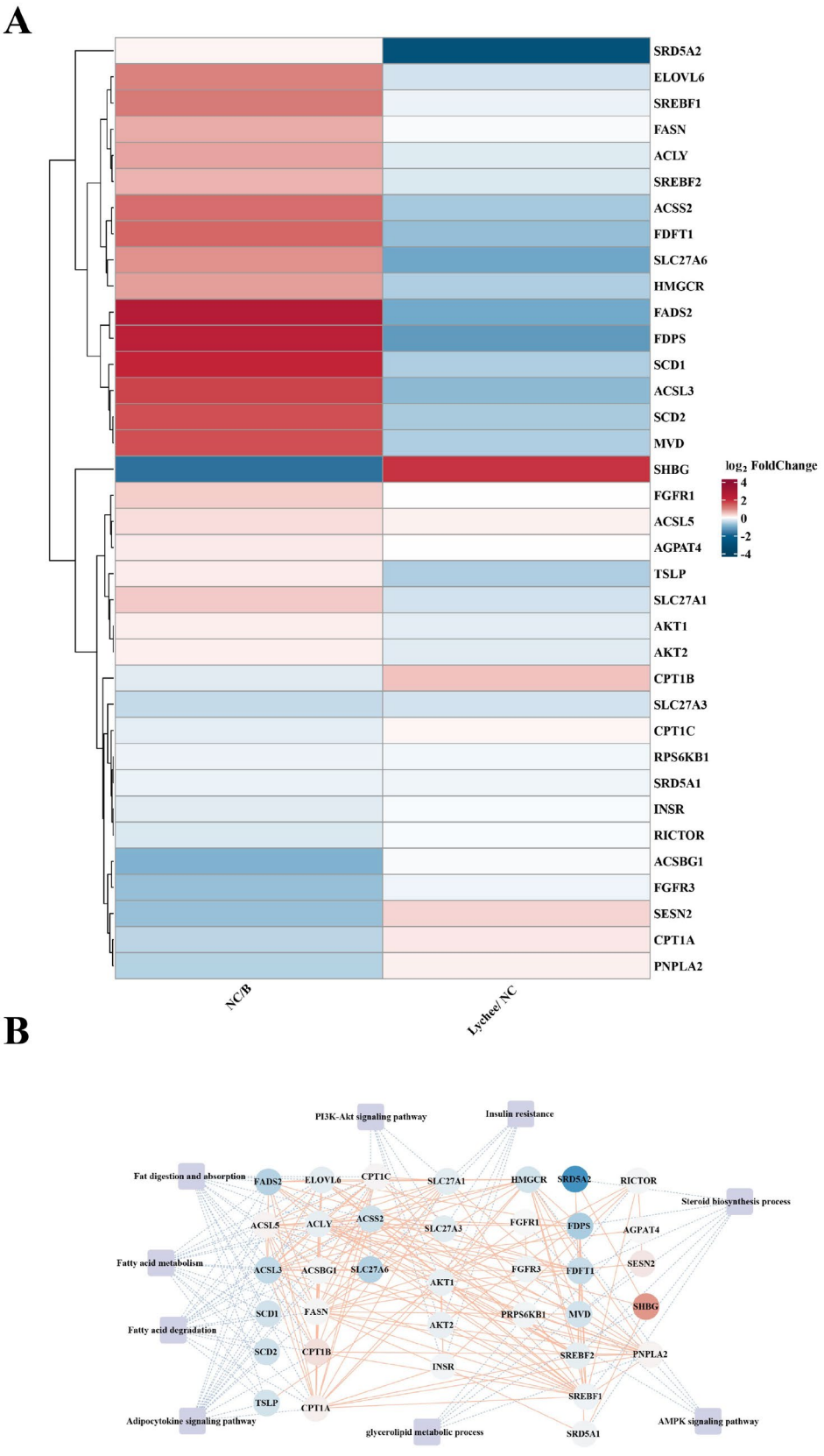


FIGURE 7 | Legend on next page.

FIGURE 7 | Statistics of key differential genes. (A) Heatmap of differential gene expression. The abscissa represents the change ratio of gene expression between different sample groups, the right ordinate represents the gene name, and the left ordinate represents the cluster analysis dendrogram of gene expression patterns, illustrating the similarity in gene expression patterns. Blue indicates that gene expression is downregulated, and red indicates that gene expression is upregulated. For this result, three independent biological replicates were performed. (B) Signal Pathway–PPI network of oil control target genes. The left and right light purple squares represent relevant signal pathways, the circle represents oil control target genes, and the blue circle represents downregulated genes, with deeper shades indicating that the gene expression is more downregulated; pink circles represent upregulated genes, and the deeper the pink, the more upregulated the gene expression.

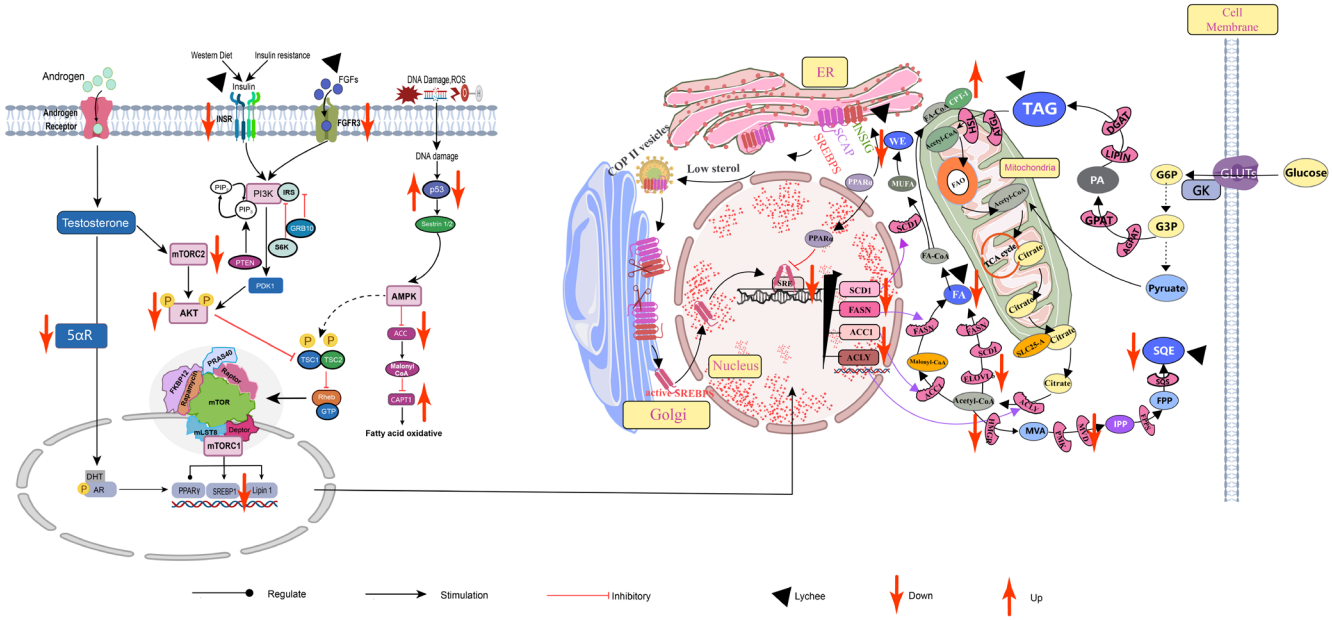


FIGURE 8 | Mechanism of Lychee's influence on lipid metabolism. In the figure, the black triangle represents Lychee, and its marked position indicates the starting point and ending point of the influence of the sample on oil secretion. The red bold arrow signifies the expression change of the coding gene corresponding to the related protein after the intervention of the sample, in which the up arrow (↑) indicates the upregulation of gene expression, and the down arrow (↓) indicates the downregulation of gene expression. On the left is the change of gene or protein induced by the sample intervention through the signal pathway, and on the right is the change of gene, which further affects fat synthesis and metabolism.

downstream signal pathways, particularly through the interplay and functional correlation of key target genes. Additionally, we annotated the sample's target to identify the regulation mechanism of the sample in skin lipid metabolism (Figure 8). RNA-seq analysis revealed that the introduction of lychee primarily modulated oil secretion from the sebaceous gland cells stimulated by linoleic acid through the regulation of fatty acid metabolism, fatty acid degradation, insulin resistance, the PI3K-Akt signaling pathway, the AMPK signaling pathway, glyceride metabolism, and associated genes. The specific mechanisms were as follows: (1) inhibition of 5α reductase activity and SRD5A2 expression, reduction of dihydrotestosterone (DHT), control of SREBP1 (Coding gene SREBF1), and inhibition of lipid synthesis; (2) inhibition of mTORC2 activity, enhancement of Forkhead box protein O1 (FoxO1) activity, activation of the AMPK pathway, inhibition of acetyl-CoA carboxylase (ACC) activity, and facilitation of fatty acid oxidation; (3) resistance to the effects of growth factors, inhibition of FGFR3 and INSR expression, downregulation of AKT1 and AKT2, negative regulation of mTORC1, and inhibition of lipid synthesis; (4) reduction of gene expression, including SREBF1, ACLY, SCD1, and FASN, and inhibition of wax fat and squalene synthesis; and (5) downregulation of SLC27A1, TSLP, and AGPAT gene expression, and regulation of fatty acid metabolism and oil secretion.

3.9 | Fluorescence Intensity Test of Cellular Oil Secretion

At a concentration of 0.1%, the fluorescence intensity of ZY2 is 11.655 ± 0.202 ($p < 0.05$), and the inhibition rate of oil secretion is 32.162% (Figure 9), which is significantly different from the negative control group, indicating that ZY2 has an oil control effect at this concentration.

4 | Discussion

This study represents the first systematic examination of the regulatory effects of *litchi* extract on cutaneous sebum secretion. Our findings indicate that among various fraction-enriched *litchi* extracts, the total flavonoid-enriched fraction (*Litchi chinensis* flavonoids, LCFs; referred to as sample ZY2) exhibited the most significant anti-inflammatory activity and efficacy in restoring oil–water balance in a mouse model of seborrheic dermatitis induced by DNCB and a high-fat diet. Therefore, we detected that LCFs mainly contain rutin, quercitrin, luteoloside, naringin, isoquercitrin, and phloridzin by HPLC. Based on these in vivo observations, we conducted transcriptomic profiling [45–47] to clarify the multi-target and multi-pathway molecular

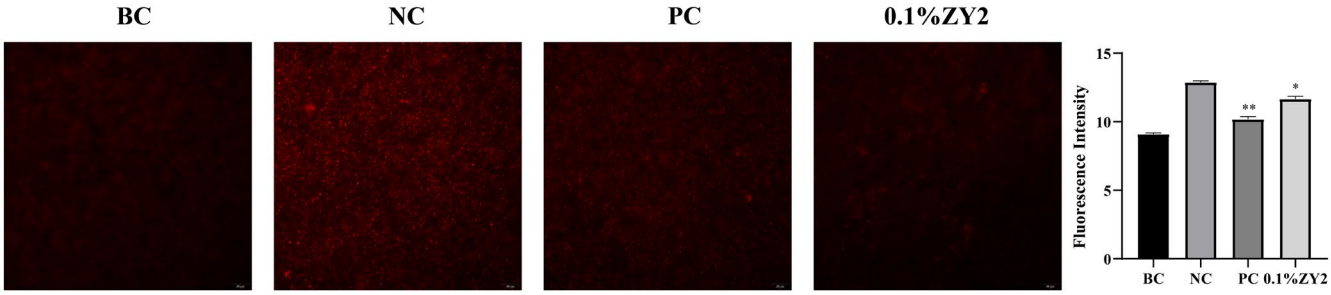


FIGURE 9 | Fluorescence intensity test results of cell lipid droplets. Red fluorescence represents lipid droplets, and the higher the intensity of red fluorescence, the more obvious it is, indicating more oil secretion. For this result, three independent biological replicates were performed. $^{**}p < 0.01$ vs the NC group. $^{*}p < 0.05$ vs the NC group.

mechanisms by which LCFs regulate sebum synthesis and secretion in a linoleic acid-induced human sebocyte (SZ95) model [48]. Finally, we detected the fluorescence intensity of cell oil secretion and found that the inhibition rate of LCFs was 32.162% at the concentration of 0.1%, which was significantly different from the negative control group, indicating that LCFs had an oil control effect at this concentration. Collectively, this work opens a new avenue for litchi—a traditional plant resource—in sebum regulation and provides novel insights into the complex molecular networks by which plant-derived flavonoids influence sebaceous gland function.

Recently, using botanical extracts to regulate sebum secretion has attracted increasing attention. For instance, guava (*Psidium guajava*) and red ginseng (*Panax ginseng*) extracts have exhibited clinical efficacy in regulating sebum production [49, 50]. Chrysophanol isolated from *Cassia torosa* seeds suppresses lipogenesis by inhibiting the JNK/p38 MAPK signaling pathway [51]. Similarly, extracts from *Cirsium eriophorum* and *Asparagus racemosus* primarily exert oil-controlling effects through the inhibition of 5α-reductase activity [52, 53]. Compared with these studies, the novelty of our work is in the finding that LCFs do not operate through a single target; instead, they exert sebum-regulatory effects through the coordinated modulation of a synergistic molecular network. Transcriptomic analysis revealed that LCFs downregulate SRD5A1 expression, and SRD5A2 modulates several core metabolic signaling pathways, including insulin resistance, PI3K-Akt–mTOR, and AMPK. These findings suggest that LCFs may have a wider and more robust potential for sebum regulation than other natural compounds.

Our RNA-seq findings elucidate the LCF-mediated regulatory blueprint at three major levels:

1. Inhibition of upstream pro-lipogenic signaling: LCFs significantly downregulated INSR, FGFR1, and FGFR3, all of which are potent stimulators of lipogenesis in sebocytes [54, 55]. By attenuating these upstream cues, LCFs reduce PI3K-Akt signaling at its origin, thereby mitigating growth factor-mediated lipid synthesis.
2. Reconfiguration of core metabolic networks: The PI3K-Akt–mTOR pathway serves as a central hub for cellular anabolism. Our data indicate that LCFs inhibit mTORC1 and mTORC2 activities, downregulate AKT1 and AKT2, and simultaneously enhance FoxO1 activity. Inhibition of mTORC1 and activation of FoxO1 together attenuate lipogenesis [56, 57]. Simultaneously, LCFs stimulate AMPK signaling by upregulating SESN1/2. AMPK functions as a cellular energy sensor by inhibiting anabolic processes (such as fatty acid synthesis) and promoting catabolic processes (such as fatty acid oxidation) [58, 59]. Accordingly, by concurrently inhibiting mTOR and activating AMPK, LCFs transform sebocytes from a lipogenic to a catabolic state.
3. Direct regulation of androgen metabolism and lipogenic genes: LCFs markedly downregulated SRD5A1 and SRD5A2, thereby diminishing the conversion of testosterone into the more potent dihydrotestosterone (DHT) and attenuating androgen-mediated sebaceous activity [53, 60]. These multi-pathway regulatory events culminate in the inhibition of the master lipogenic transcription factor SREBF1. SREBF1 downregulation resulted in a significant decrease in its downstream targets, including ACLY, FASN, and SCD1 (*de novo* fatty acid synthesis), SLC27A1 (fatty acid transport), and AGPAT (triglyceride synthesis) [1, 61–65]. These changes collectively establish a comprehensive inhibition of sebum production at the executive level.

We proposed a comprehensive model of LCF-mediated sebum regulation based on these findings (Figures 7 and 8). This concept posits that LCFs mitigate diet-induced insulin resistance and excessive growth factor stimulation, thereby altering the PI3K-Akt–mTOR/AMPK/SREBF1 signaling pathway and inhibiting pathological sebum overproduction [14, 66]. This process is highly relevant to the pathophysiology of adolescent acne, where hormonal fluctuations and high-glycemic diets hyperactivate sebaceous glands through androgen signaling, exacerbate insulin resistance, and PI3K-Akt–mTOR pathway overactivation [67–70]. The ability of LCFs to target these key pathogenic mechanisms highlights their promising potential in preventing and mitigating oily skin conditions, including adolescent acne.

As a natural, plant-derived ingredient, LCFs may offer enhanced safety and lower risk of side effects during long-term use compared with conventional chemical drugs (retinoids and antibiotics). Consequently, they represent a promising option for integration into daily skincare formulations. This study has some

limitations. First, we mainly rely on transcriptomics data to infer its mechanism of action, which is instructive [46, 71]. For example, Sergio Acin et al. [72] found that the extract of *Eucalyptus tereticornis* regulated the expression of genes involved in lipogenesis, lipolysis, and extracellular matrix remodeling by transcriptomics. However, further functional experiments are needed to verify the expression changes of key targets at the protein level (such as Western Blot). Second, only linoleic acid was used as an inducer in vitro; future studies should integrate other stimuli, including insulin and DHT, to better mimic the complex physiological and pathological environment of sebaceous glands.

In conclusion, this study presents the first evidence that total flavonoids from *Litchi chinensis* (LCFs) exert significant oil–water balance-restoring effects in vivo and suppress sebum secretion in vitro. Transcriptomic analysis demonstrated that LCFs operate through a multi-target, multi-pathway mechanism, synergistically modulating 5α-reductase activity, PI3K-Akt–mTOR and AMPK pathways, and the SREBF1-driven lipid synthesis network. These findings fill a critical gap in the application of *litchi*-derived compounds for sebum regulation and provide a robust scientific basis for the development of safe, effective, and naturally sourced sebum-controlling agents. This study offers a novel perspective and potential therapeutic approach for managing sebum-related skin disorders, especially in adolescents.

Author Contributions

Qinqian Tao: conceptualization, data curation, methodology, writing – original draft, writing – review and editing, supervision, and project administration. **Xingmei Chen:** formal analysis, investigation, validation, data curation, writing – original draft and visualization. **Xian Chen:** formal analysis, investigation, software and validation. **Xiang Yang:** investigation, validation and data curation. **Erping Yan:** conceptualization, methodology, supervision, project administration, and writing – review and editing. All authors have read and agreed to the published version of the manuscript.

Funding

The authors have nothing to report.

Ethics Statement

The Bioethics Committee of East China University of Science (ECUST-2023-001) approved all animal procedures, which were performed in accordance with relevant guidelines and regulations.

Conflicts of Interest

The authors declare no conflicts of interest.

Data Availability Statement

The data that support the findings of this study are available from the corresponding author upon reasonable request.

References

1. M. Schmidt, H. Binder, and M. R. Schneider, "The Metabolic Underpinnings of Sebaceous Lipogenesis," *Communications Biology* 8, no. 1 (2025): 670, https://doi.org/10.1038/s42003-025-08105-9.

2. L. Shuo, Y. Ting, W. KeLun, Z. Rui, Z. Rui, and W. Hang, "Efficacy and Possible Mechanisms of Botulinum Toxin Treatment of Oily Skin," *Journal of Cosmetic Dermatology* 18, no. 2 (2019): 451–457, https://doi.org/10.1111/jocd.12866.

3. G. Shamloul and A. Khachemoune, "An Updated Review of the Sebaceous Gland and Its Role in Health and Diseases Part 1: Embryology, Evolution, Structure, and Function of Sebaceous Glands," *Dermatologic Therapy* 34, no. 1 (2021): e14695, https://doi.org/10.1111/dth.14695.

4. S. Eyerich, K. Eyerich, C. Traidl-Hoffmann, and T. Biedermann, "Cutaneous Barriers and Skin Immunity: Differentiating a Connected Network," *Trends in Immunology* 39, no. 4 (2018): 315–327, https://doi.org/10.1016/j.it.2018.02.004.

5. J. Y. Hong, S. J. Park, S. J. Seo, and K. Y. Park, "Oily Sensitive Skin: A Review of Management Options," *Journal of Cosmetic Dermatology* 19, no. 5 (2020): 1016–1020, https://doi.org/10.1111/jocd.13347.

6. J. Wei, X. Ma, M. Chen, S. Pan, and Y. Pang, "In Vitro and In Vivo Study of the Efficacy of a New Sebum Control Essence," *Journal of Cosmetic Dermatology* 22, no. 9 (2023): 2605–2611, https://doi.org/10.1111/jocd.15764.

7. X. Zhang, Z. Zhang, H. Tao, et al., "Comprehensive Assessment of the Efficacy and Safety of a Clay Mask in Oily and Acne Skin," *Skin Research and Technology* 29, no. 11 (2023): e13513, https://doi.org/10.1111/srt.13513.

8. D. J. Jo, J. Y. Shin, and S. J. Na, "Evaluation of Changes for Sebum, Skin Pore, Texture, and Redness Before and After Sleep in Oily and Nonoily Skin," *Skin Research and Technology* 28, no. 6 (2022): 851–855, https://doi.org/10.1111/srt.13224.

9. M. Gabarra Almeida Leite and P. M. B. G. Maia Campos, "Correlations Between Sebaceous Glands Activity and Porphyrins in the Oily Skin and Hair and Immediate Effects of Dermocosmetic Formulations," *Journal of Cosmetic Dermatology* 19, no. 11 (2020): 3100–3106, https://doi.org/10.1111/jocd.13370.

10. R. Dhurat, D. Shukla, R. K. Lim, C. G. Wambier, and A. Goren, "Spironolactone in Adolescent Acne Vulgaris," *Dermatologic Therapy* 34, no. 1 (2021): e14680, https://doi.org/10.1111/dth.14680.

11. I. C. Valente Duarte De Sousa, "New and Emerging Drugs for the Treatment of Acne Vulgaris in Adolescents," *Expert Opinion on Pharmacotherapy* 20, no. 8 (2019): 1009–1024, https://doi.org/10.1080/14656566.2019.1584182.

12. G. Yosipovitch, M. Tang, A. G. Dawn, et al., "Study of Psychological Stress, Sebum Production and Acne Vulgaris in Adolescents," *Acta Dermato-Venereologica* 87, no. 2 (2007): 135–139, https://doi.org/10.2340/00015555-0231.

13. Z. Jin, Y. Song, and L. He, "A Review of Skin Immune Processes in Acne," *Frontiers in Immunology* 14 (2023): 1324930, https://doi.org/10.3389/fimmu.2023.1324930.

14. B. C. Melnik, "Acne Transcriptomics: Fundamentals of Acne Pathogenesis and Isotretinoin Treatment," *Cells* 12, no. 22 (2023): 2600, https://doi.org/10.3390/cells12222600.

15. Ö. Kutlu, A. S. Karadağ, and U. Wollina, "Adult Acne Versus Adolescent Acne: A Narrative Review With a Focus on Epidemiology to Treatment," *Anais Brasileiros de Dermatologia* 98, no. 1 (2023): 75–83, https://doi.org/10.1016/j.abd.2022.01.006.

16. K. Mansoor, T. Aburjai, F. Al-Mamoori, and M. Schmidt, "Plants With Cosmetic Uses," *Phytotherapy Research* 37, no. 12 (2023): 5755–5768, https://doi.org/10.1002/ptr.8019.

17. G. Das, S. Kameswaran, B. Ramesh, et al., "Anti-Aging Effect of Traditional Plant-Based Food: An Overview," *Food* 13, no. 23 (2024): 3785, https://doi.org/10.3390/foods13233785.

18. E. F. Costa, W. V. Magalhães, and L. C. Di Stasi, "Recent Advances in Herbal-Derived Products With Skin Anti-Aging Properties and

Cosmetic Applications," *Molecules* 27, no. 21 (2022): 7518, https://doi.org/10.3390/molecules27217518.

19. J. Olivero-Verbel, P. Quintero-Rincón, and K. Caballero-Gallardo, "Aromatic Plants as Cosmeceuticals: Benefits and Applications for Skin Health," *Planta* 260, no. 6 (2024): 132, https://doi.org/10.1007/s00425-024-04550-8.

20. E. Roh, J. Kim, J. Y. Kwon, et al., "Molecular Mechanisms of Green Tea Polyphenols With Protective Effects Against Skin Photoaging," *Critical Reviews in Food Science and Nutrition* 57, no. 8 (2017): 1631–1637, https://doi.org/10.1080/10408398.2014.1003365.

21. M. S. Ferreira, M. C. Magalhães, R. Oliveira, J. M. Sousa-Lobo, and I. F. Almeida, "Trends in the Use of Botanicals in Anti-Aging Cosmetics," *Molecules* 26, no. 12 (2021): 3584, https://doi.org/10.3390/molecules26123584.

22. F. Farjadmand, E. Karimpour-Razkenari, S. M. Nabavi, M. R. S. Ardekani, and M. Saeedi, "Plant Polyphenols: Natural and Potent UV-Protective Agents for the Prevention and Treatment of Skin Disorders," *Mini-Reviews in Medicinal Chemistry* 21, no. 5 (2021): 576–585, https://doi.org/10.2174/1389557520666201109121246.

23. M. Michalak, "Plant-Derived Antioxidants: Significance in Skin Health and the Ageing Process," *International Journal of Molecular Sciences* 23, no. 2 (2022): 585, https://doi.org/10.3390/ijms23020585.

24. M. Yang, L. Tao, Z. Wang, et al., "The Mechanism of Peach Gum Polysaccharide Preventing UVB-Induced Skin Photoaging by Regulating Matrix Metalloproteinanse and Oxidative Factors," *Molecules* 28, no. 10 (2023): 4104, https://doi.org/10.3390/molecules28104104.

25. W. Du, Z. Wang, M. Han, et al., "Astragalus Polysaccharide-Containing 3D-Printed Scaffold for Traumatized Skin Repair and Proteomic Study," *Journal of Cellular and Molecular Medicine* 28, no. 16 (2024): e70023, https://doi.org/10.1111/jcmm.70023.

26. M. Zhao, J. Xiang, Y. Meng, et al., "Astragalus Polysaccharide Hydrogels With Drug-Carrying Super Self-Assembly From Natural Herbs Promote Wound Healing," *ACS Nano* 19, no. 23 (2025): 21571–21588, https://doi.org/10.1021/acsnano.5c03744.

27. Y. Liu, J. Liu, R. Xu, et al., "*Ludwigia adscendens* (L.) Hara Extract Inhibits Sebum Overproduction and Improves Sebaceous Gland Function via the PPARγ/LXRα/SREBP1 Pathway," *Journal of Ethnopharmacology* 353, no. Pt B (2025): 120416, https://doi.org/10.1016/j.jep.2025.120416.

28. J. Y. Yoon, H. H. Kwon, S. U. Min, D. M. Thiboutot, and D. H. Suh, "Epigallocatechin-3-Gallate Improves Acne in Humans by Modulating Intracellular Molecular Targets and Inhibiting *P. acnes*," *Journal of Investigative Dermatology* 133, no. 2 (2013): 429–440, https://doi.org/10.1038/jid.2012.292.

29. K. Lee, J. Youm, W. J. Lee, S. Kang, and Y. J. Kim, "Polyphenol-Rich Apple Extract Inhibits Dexamethasone-Induced Sebaceous Lipids Production by Regulating SREBP1 Expression," *Experimental Dermatology* 26, no. 10 (2017): 958–960, https://doi.org/10.1111/exd.13319.

30. Y. Tu, N. Li, H. Liu, D. Sun, L. He, and H. Gu, "Polysaccharide From *Prinsepia utilis* Royle Maintains the Skin Barrier by Mediating Differentiation, Lipid Metabolism and Tight Junction of Keratinocyte," *Scientific Reports* 15, no. 1 (2025): 20470, https://doi.org/10.1038/s41598-025-01960-w.

31. L. Cheng, J. Guo, and Y. Lu, "Inhibition of Lipogenesis and Sebum Secretion for *Lotus corniculatus* Seed Extract In Vitro and In Vivo," *International Journal of Cosmetic Science* 45, no. 1 (2023): 62–72, https://doi.org/10.1111/ics.12823.

32. J. Lora and J. Hormaza, "Genetics and Breeding of Fruit Crops in the Sapindaceae Family: Lychee (*Litchi chinensis* Sonn.) and Longan (*Dimocarpus longan* Lour.)," (2018).

33. S. R. M. Ibrahim and G. A. Mohamed, "*Litchi chinensis*: Medicinal Uses, Phytochemistry, and Pharmacology," *Journal of Ethnopharmacology* 174 (2015): 492–513, https://doi.org/10.1016/j.jep.2015.08.054.

34. K. Huang, D. Fu, Y. Jiang, et al., "Storability and Linear Regression Models of Pericarp Browning and Decay in Fifty Litchi (*Litchi chinensis* Sonn.) Cultivars at Room Temperature Storage," *Food* 12, no. 8 (2023): 1725, https://doi.org/10.3390/foods12081725.

35. X. Zhang, L. Zhao, W. Zhou, X. Liu, Z. Hu, and K. Wang, "Variations in the Multilevel Structure, Gelatinization and Digestibility of Litchi Seed Starches From Different Varieties," *Food* 11, no. 18 (2022): 2821, https://doi.org/10.3390/foods11182821.

36. W. Gao, P. Lin, X. Zeng, and M. A. Brennan, "Preparation, Characterisation and Antioxidant Activities of Litchi (*Litchi chinensis* Sonn.) Polysaccharides Extracted by Ultra-High Pressure," *International Journal of Food Science and Technology* 52, no. 8 (2017): 1739–1750, https://doi.org/10.1111/ijfs.13447.

37. X. Zhu, H. Wang, J. Sun, B. Yang, X. Duan, and Y. Jiang, "Pericarp and Seed of Litchi and Longan Fruits: Constituent, Extraction, Bioactive Activity, and Potential Utilization," *Journal of Zhejiang University. Science. B* 20, no. 6 (2019): 503–512, https://doi.org/10.1631/jzus.B1900161.

38. S. Emanuele, M. Lauricella, G. Calvaruso, A. D'Anneo, and M. Giuliano, "*Litchi chinensis* as a Functional Food and a Source of Antitumor Compounds: An Overview and a Description of Biochemical Pathways," *Nutrients* 9, no. 9 (2017): 992, https://doi.org/10.3390/nu9090992.

39. N. Lourith and M. Kanlayavattanakul, "Formulation and Clinical Evaluation of the Standardized *Litchi chinensis* Extract for Skin Hyperpigmentation and Aging Treatments," *Annales Pharmaceutiques Françaises* 78, no. 2 (2020): 142–149, https://doi.org/10.1016/j.pharma.2020.01.004.

40. C. I. Cano-Gómez, A. J. Alonso-Castro, C. Carranza-Alvarez, and J. E. Wong-Paz, "Advancements in *Litchi chinensis* Peel Processing: A Scientific Review of Drying, Extraction, and Isolation of Its Bioactive Compounds," *Food* 13, no. 10 (2024): 1461, https://doi.org/10.3390/foods13101461.

41. L. C. Thiesen, T. Baccarin, A. F. Fischer-Muller, et al., "Photochemoprotective Effects Against UVA and UVB Irradiation and Photosafety Assessment of *Litchi chinensis* Leaves Extract," *Journal of Photochemistry and Photobiology, B: Biology* 167 (2017): 200–207, https://doi.org/10.1016/j.jphotobiol.2016.12.033.

42. A. García-Villegas, A. Rojas-García, M. D. C. Villegas-Aguilar, et al., "Cosmeceutical Potential of Major Tropical and Subtropical Fruit By-Products for a Sustainable Revalorization," *Antioxidants* 11, no. 2 (2022): 203, https://doi.org/10.3390/antiox11020203.

43. M. Garber, M. G. Grabherr, M. Guttman, and C. Trapnell, "Computational Methods for Transcriptome Annotation and Quantification Using RNA-Seq," *Nature Methods* 8, no. 6 (2011): 469–477, https://doi.org/10.1038/nmeth.1613.

44. L. D. Goldstein, Y. Cao, G. Pau, et al., "Prediction and Quantification of Splice Events From RNA-Seq Data," *PLoS One* 11, no. 5 (2016): e156132, https://doi.org/10.1371/journal.pone.0156132.

45. X. Gu, "Statistical Detection of Differentially Expressed Genes Based on RNA-Seq: From Biological to Phylogenetic Replicates," *Briefings in Bioinformatics* 17, no. 2 (2016): 243–248, https://doi.org/10.1093/bib/bbv035.

46. W. K. Cho, S. H. Paek, S. Kim, et al., "Comparative Transcriptome Profiles of Human HaCaT Cells in Response to *Gynostemma pentaphyllum* Extracts Obtained Using Three Independent Methods by RNA Sequencing," *Life-Basel* 13, no. 2 (2023): 423, https://doi.org/10.3390/life13020423.

47. W. K. Cho, S. Kim, S. J. Jang, et al., "Comparative Analysis of Water Extracts From Roselle (*Hibiscus sabdariffa* L.) Plants and Callus Cells: Constituents, Effects on Human Skin Cells, and Transcriptome Profiles," *International Journal of Molecular Sciences* 24, no. 13 (2023): 10853, https://doi.org/10.3390/ijms241310853.

48. D. Kovács, E. Camera, S. Póliska, et al., "Linoleic Acid Induced Changes in SZ95 Sebocytes-Comparison With Palmitic Acid and

Arachidonic Acid," *Nutrients* 15, no. 15 (2023): 3315, https://doi.org/10.3390/nu15153315.

49. P. Pongsakornpaisan, N. Lourith, and M. Kanlayavattanakul, "Anti-Sebum Efficacy of Guava Toner: A Split-Face, Randomized, Single-Blind Placebo-Controlled Study," *Journal of Cosmetic Dermatology* 18, no. 6 (2019): 1737–1741, https://doi.org/10.1111/jocd.12943.

50. J. H. Hou, H. Shin, K. H. Jang, et al., "Anti-Acne Properties of Hydrophobic Fraction of Red Ginseng (*Panax ginseng* C.A. Meyer) and Its Active Components," *Phytotherapy Research* 33, no. 3 (2019): 584–590, https://doi.org/10.1002/ptr.6243.

51. H. C. Kwon, T. Y. Kim, C. M. Lee, K. S. Lee, and K. K. Lee, "Active Compound Chrysophanol of *Cassia tora* Seeds Suppresses Heat-Induced Lipogenesis via Inactivation of JNK/p38 MAPK Signaling in Human Sebocytes," *Lipids in Health and Disease* 18, no. 1 (2019): 135, https://doi.org/10.1186/s12944-019-1072-x.

52. S. Laneri, I. Dini, A. Tito, et al., "Plant Cell Culture Extract of *Cirsium eriophorum* With Skin Pore Refiner Activity by Modulating Sebum Production and Inflammatory Response," *Phytotherapy Research* 35, no. 1 (2021): 530–540, https://doi.org/10.1002/ptr.6832.

53. W. Ruksiriwanich, C. Khantham, P. Linsaenkart, et al., "In Vitro and In Vivo Regulation of SRD5A mRNA Expression of Supercritical Carbon Dioxide Extract From Asparagus Racemosus Willd. Root as Anti-Sebum and Pore-Minimizing Active Ingredients," *Molecules* 27, no. 5 (2022): 1535, https://doi.org/10.3390/molecules27051535.

54. Z. Xu, J. Huang, M. Wen, et al., "Gentiopicroside Ameliorates Glucose and Lipid Metabolism in T2DM via Targeting FGFR1," *Phytomedicine* 132 (2024): 155780, https://doi.org/10.1016/j.phymed.2024.155780.

55. Y. Chu, S. Yang, and X. Chen, "Fibroblast Growth Factor Receptor Signaling in Metabolic Dysfunction-Associated Fatty Liver Disease: Pathogenesis and Therapeutic Targets," *Pharmacology & Therapeutics* 269 (2025): 108844, https://doi.org/10.1016/j.pharmthera.2025.108844.

56. S. M. Jung, C. Hung, S. R. Hildebrand, et al., "Non-Canonical mTORC2 Signaling Regulates Brown Adipocyte Lipid Catabolism Through SIRT6-FoxO1," *Molecular Cell* 75, no. 4 (2019): 807–822, https://doi.org/10.1016/j.molcel.2019.07.023.

57. A. Szwed, E. Kim, and E. Jacinto, "Regulation and Metabolic Functions of mTORC1 and mTORC2," *Physiological Reviews* 101, no. 3 (2021): 1371–1426, https://doi.org/10.1152/physrev.00026.2020.

58. L. Gong, Z. Wang, Z. Wang, and Z. Zhang, "Sestrin2 as a Potential Target for Regulating Metabolic-Related Diseases," *Frontiers in Endocrinology* 12 (2021): 751020, https://doi.org/10.3389/fendo.2021.751020.

59. Y. Ma, G. Zhang, Z. Kuang, et al., "Empagliflozin Activates Sestrin2-Mediated AMPK/mTOR Pathway and Ameliorates Lipid Accumulation in Obesity-Related Nonalcoholic Fatty Liver Disease," *Frontiers in Pharmacology* 13 (2022): 944886, https://doi.org/10.3389/fphar.2022.944886.

60. É. Audet-Walsh, T. Yee, I. S. Tam, and V. Giguère, "Inverse Regulation of DHT Synthesis Enzymes 5α-Reductase Types 1 and 2 by the Androgen Receptor in Prostate Cancer," *Endocrinology* 158, no. 4 (2017): 1015–1021, https://doi.org/10.1210/en.2016-1926.

61. H. Liu, C. Wei, Y. Chen, Y. Chen, and S. Chang, "Flavanol-Rich Lychee Fruit Extract Alleviates Diet-Induced Insulin Resistance via Suppressing mTOR/SREBP-1 Mediated Lipogenesis in Liver and Restoring Insulin Signaling in Skeletal Muscle," *Molecular Nutrition & Food Research* 60, no. 10 (2016): 2288–2296, https://doi.org/10.1002/mnfr.201501064.

62. X. Feng, L. Zhang, S. Xu, and A. Shen, "ATP-Citrate Lyase (ACLY) in Lipid Metabolism and Atherosclerosis: An Updated Review," *Progress in Lipid Research* 77 (2020): 101006, https://doi.org/10.1016/j.plipres.2019.101006.

63. C. Ji, Y. Guo, Y. Liu, et al., "Inhibition of Ceramide De Novo Synthesis Ameliorates Meibomian Gland Dysfunction Induced by SCD1 Deficiency," *Ocular Surface* 22 (2021): 230–241, https://doi.org/10.1016/j.jtos.2021.08.016.

64. Y. Xiao, Y. Yang, H. Xiong, and G. Dong, "The Implications of FASN in Immune Cell Biology and Related Diseases," *Cell Death & Disease* 15, no. 1 (2024): 88, https://doi.org/10.1038/s41419-024-06463-6.

65. H. Wang, M. V. Airola, and K. Reue, "How Lipid Droplets 'TAG' Along: Glycerolipid Synthetic Enzymes and Lipid Storage," *Biochimica et Biophysica Acta-Molecular and Cell Biology of Lipids* 1862, no. 10 Pt B (2017): 1131–1145, https://doi.org/10.1016/j.bbalip.2017.06.010.

66. Y. Li, X. Hu, G. Dong, X. Wang, and T. Liu, "Acne Treatment: Research Progress and New Perspectives," *Frontiers in Medicine* 11 (2024): 1425675, https://doi.org/10.3389/fmed.2024.1425675.

67. R. W. Clayton, K. Göbel, C. M. Niessen, R. Paus, M. A. M. van Steensel, and X. Lim, "Homeostasis of the Sebaceous Gland and Mechanisms of Acne Pathogenesis," *British Journal of Dermatology* 181, no. 4 (2019): 677–690, https://doi.org/10.1111/bjd.17981.

68. R. W. Clayton, E. A. Langan, D. M. Ansell, et al., "Neuroendocrinology and Neurobiology of Sebaceous Glands," *Biological Reviews* 95, no. 3 (2020): 592–624, https://doi.org/10.1111/brv.12579.

69. H. Gu, H. An, M. Gwon, S. Bae, C. C. Zouboulis, and K. Park, "The Effects of Synthetic SREBP-1 and PPAR-γ Decoy Oligodeoxynucleotide on Acne-Like Disease In Vivo and In Vitro via Lipogenic Regulation," *Biomolecules* 12, no. 12 (2022): 1858, https://doi.org/10.3390/biom12121858.

70. S. Cruz, N. Vecerek, and N. Elbuluk, "Targeting Inflammation in Acne: Current Treatments and Future Prospects," *American Journal of Clinical Dermatology* 24, no. 5 (2023): 681–694, https://doi.org/10.1007/s40257-023-00789-1.

71. N. L. Bray, H. Pimentel, P. Melsted, and L. Pachter, "Near-Optimal Probabilistic RNA-Seq Quantification," *Nature Biotechnology* 34, no. 5 (2016): 525–527, https://doi.org/10.1038/nbt.3519.

72. S. Acin, A. Mejia-Garcia, G. J. Fernandez, and N. Balcazar, "A Triterpene-Enriched Natural Extract From *Eucalyptus tereticornis* Modulates the Expression of Genes Involved in Adipogenesis, Lipolysis, and Extracellular Matrix Remodeling in a Primary Human and Mouse Cell Line Adipocyte," *Pharmaceutical Biology* 63, no. 1 (2025): 374–386, https://doi.org/10.1080/13880209.2025.2505443.